ACS OMEGA

Open Access

http://pubs.acs.org/journal/acsodf

Article

Derivatives of Pyrazole-Based Compounds as Prospective Cancer Agents

Lesetja V. Ramoba, Wakopo J. Nzondomyo, Karabo Serala, Lucy W. Macharia, Supratim Biswas, Sharon Prince, Frederick P. Malan, Orbett T. Alexander, and Amanda-Lee E. Manicum*

Cite This: *ACS Omega* 2025, 10, 12671−12678

Read Online

ACCESS | Metrics & More | Article Recommendations | Supporting Information

ABSTRACT: Five pyrazole-based compounds, 3,5-dimethyl-1*H*-pyrazole, **L1**; 3,5-diphenyl-1*H*-pyrazole, **L2**; 3-(trifluoromethyl)-5-phenyl-1*H*-pyrazole, **L3**; 3-(trifluoromethyl)-5-methyl-1*H*-pyrazole, **L4**; and 3,5-ditert-butyl-1*H*-pyrazole, **L5** were synthesized from a typical condensation reaction of β-diketone derivatives with hydrazine hydrate reagent and characterized using various spectroscopic techniques such as FT-IR, UV−vis, ^{1}H and ^{13}C NMR, and LC−MS spectroscopy. **L1** was further analyzed by single-crystal X-ray diffraction, and the N1−N1′ bond distance was found to be 1.361(3) Å and correlated well with other pyrazole-based compounds. The short-term cytotoxicity of 10 μM pyrazole compounds (**L1**−**L5**) was evaluated against pancreatic (CFPAC-1 and PANC-1), breast (MDA-MB-231 and MCF-7), and cervical (CaSki and HeLa) cancer cell lines using the MTT cell viability assay. Cisplatin and gemcitabine were included as positive control drugs followed by the determination of the half-maximal effective concentrations of prospective compounds. **L2** and **L3**, respectively, displayed moderate cytotoxicity against CFPAC-1 (61.7 ± 4.9 μM) and MCF-7 (81.48 ± 0.89 μM) cell lines.

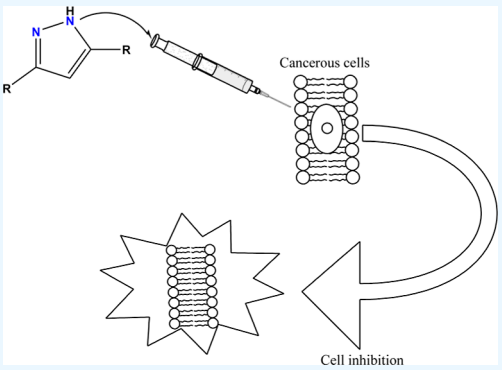

1. INTRODUCTION

Pyrazoles are five-membered heterocyclic compounds derived from a simple acid-catalyzed condensation reaction of β-diketone and hydrazine derivatives and are usually synthesized using a method introduced by Knorr (1883).[1] Since the inception of his procedure, alternative synthetic pathways to obtain pyrazole compounds have been developed through numerous modifications of the method by the aforementioned pioneer. One of the modified procedures was conducted by Girish and co-workers,[2] where they used a nano-ZnO catalyst for the synthesis of 1,3,5-substituted pyrazole derivatives. The main advantages of this protocol are the high yield (95%) and reduced reaction time, which are almost similar to the method employed in this study. The other method that can also be considered is the one brought forward by Huang and Katzenellenbogen,[3] where a series of 4-alkyl-1,3,5-triarylpyrazoles in a regioselective fashion through the oxidation of pyrazolines were synthesized. The method first involves the preparation of pyrazolines via a cyclocondensation reaction between phenyl and 4-methoxyphenylhydrazine and chalcones, followed by alkylation at the C-4 position of the pyrazoline ring. The setback about this method, in contrast to the one employed in this study, is that it involves multiple steps prior to the final product as compared to the one-pot synthesis. Their structures involve the −C═N− functional group incorporated in a ring moiety with adjacent electron pair-bearing nitrogen atoms, whose basicity can be influenced by substituents on the ring backbone.[4−6] These compounds are useful precursors for the synthesis of many heterocyclic products such as 1-aryl-1*H*-pyrazole derivative or as chelator ligands for the preparation of coordination compounds.[7−10] In particular, the presence of the −C═N− functional moiety with two lone pairs of electrons on the nitrogen atoms makes these types of compounds significant in coordination and medicinal chemistry.[11−15] A wide range of pharmacological activities of pyrazole compounds has been reported in the literature, including antibacterial, antifungal, anti-inflammatory, and anticancer properties for the treatment of various biological health concerns.[16−23] Similar to pyrazole derivatives synthesized in this study, 4,5-dihydro-2*H*-pyrazole-2-hydroxyphenyl derivatives, namely, (1-(5-(5-chloro-2-hydroxyphenyl)-3-(*p*-tolyl)-4,5-dihydro-1*H*-pyrazol-1-yl)ethanone) and (1-(3-(4-chlorophenyl)-5-(3,5-dibromo-2-hydroxyphenyl)-4,5-dihydro-1*H*-pyrazol-1-yl)ethanone), synthesized from hydrazine hydrate and chalcones by Liu et al. (2012) showed remarkable antiproliferative effects against WM266.5 (human melanoma cell line) and MCF-7 (human breast cancer cell line). The

Received: January 27, 2025
Revised: February 19, 2025
Accepted: February 24, 2025
Published: March 20, 2025

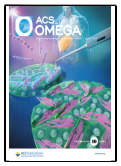

reported IC_{50} values for (1-(5-(5-chloro-2-hydroxyphenyl)-3-(*p*-tolyl)-4,5-dihydro-1*H*-pyrazol-1-yl)ethanone) were, respectively, 1.31 and 0.45 μM against MCF-7 and WM266.5 and 0.97 and 0.72 μM against MCF-7 and WM266.5 for (1-(3-(4-chlorophenyl)-5-(3,5-dibromo-2-hydroxyphenyl)-4,5-dihydro-1*H*-pyrazol-1-yl)ethanone).[24] Due to the ability of pyrazoles to form stable complexes with metal ions, numerous pyrazole-based complexes exhibit excellent catalytic activity in various reactions. Over the past few years, there have been many research studies on their applications in homogeneous and heterogeneous catalysis.[25−27]

Based on the above literature information, we decided to synthesize a series of derivatized pyrazole compounds: 3,5-dimethyl-1*H*-pyrazole, **L1**; 3,5-diphenyl-1*H*-pyrazole, **L2**; 3-(trifluoromethyl)-5-phenyl-1*H*-pyrazole, **L3**; 3-(trifluoromethyl)-5-methyl-1*H*-pyrazole, **L4**; and 3,5−3,5-ditert-butyl-1*H*-pyrazole, **L5**. The compounds were characterized using various spectroscopic techniques such as FT-IR, UV−vis, ^{1}H and ^{13}C NMR, and LC−MS. Furthermore, the crystallographic analysis on **L1** gives an insight on the pyrazole solid-state intermolecular interactions, which highlights the observed high stability of these compounds through the observed dense hydrogen bonding network in the asymmetric unit cell. Additionally, the anticancer activities of the synthesized pyrazole compounds were investigated on different cancer cell lines to assess their potential cytotoxicity. The synthesized pyrazole derivatives, due to their understood strong coordinating abilities, will at a later stage be used for chelation to the rhenium tricarbonyl metal ion to evaluate the sensitization of these compounds toward the inert *fac*-$[Re(CO)_3]^+$ synthon.

2. EXPERIMENTAL SECTION

2.1. Materials and Methods. The following chemicals pentane-2,4-dione; 2,2,6,6-tetramethylheptane-3,5-dione; 1,1,1-trifluoropentane-2,4-dione; 1,5-diphenylacetylacetone; 4,4,4-trifluoro-1-phenylbutane-1,3-dione; hydrazine hydrate; and organic solvent (ethanol) used to synthesize the pyrazole compounds were purchased from Sigma-Aldrich and were used without any further purification. ^{1}H and ^{13}C NMR spectra were determined in $CDCl_3$ and DMSO-d_6 with an internal TMS standard using a 300 MHz Bruker Avance spectrometer. The UV−vis and IR data were obtained using PerkinElmer UV−vis and FT-IR spectrophotometers, respectively.

2.2. Synthesis of the Pyrazole-Based Compounds. The reported pyrazole compounds were synthesized according to the published procedure detailed by Knorr et al. (1883).[1] They were synthesized from a simple condensation reaction of various β-diketone derivatives and hydrazine hydrate in ethanol at refluxing temperatures for the successful substitution of the carbonyl groups by amine analogues. 5.00 mL (26.3 mmol) of hydrazine hydrate was added dropwise to an equivalent amount (1:1) of various β-diketone (pentane-2,4-dione; 2,2,6,6-tetramethylheptane-3,5-dione; 1,1,1-trifluoropentane-2,4-dione; 1,5-diphenylacetylacetone; and 4,4,4-trifluoro-1-phenylbutane-1,3-dione) derivatives in 20 mL of ethanol (Scheme 1). The reaction was refluxed for 7 h, and the precipitates that formed were filtered and washed with cold ethanol, followed by drying of the solids. White cuboid crystals suitable for single-crystal X-ray diffraction were collected and analyzed for **L1**, **L2**, **L3**, and **L5**; however, only the crystal structure of **L1** is reported since the other structures are already reported in the literature.

Scheme 1. Illustration of the Synthesized Pyrazole Compounds, L1−L5

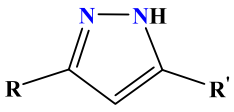

L1: R, R' = -CH_3
L2: R, R' = Ph
L3: R = Ph, R' = -CF_3
L4: R = -CH_3, R' = -CF_3
L5: R, R' = -$C(CH_3)_3$

*2.2.1. Synthesis of 3,5-Dimethyl-1H-pyrazole, **L1**.* IR $\nu_{C=N}$ (cm^{-1}) = 1600, ν_{N-N} (cm^{-1}) = 1148; ^{13}C NMR ($CDCl_3$): δ_C (ppm) (−C═N−) 144.2, (═$C_{(methine)}$−) 103.9, (−$C_{(methyl)}$) 12.1; ^{1}H NMR (400 MHz, $CDCl_3$) δ_H (N−H) 12.38 (s, 1H), (−C═CH−) 5.83 (s, 1H), (−CH_3) 2.31 (s, 6H); UV−vis: λ_{max} = 218 nm, ε [0.0018 M] = 435 $M^{-1}\cdot cm^{-1}$, LC−MS: *m*/*z* = found: 97.0759 ([M + H]$^+$), 98.0814 ([M + 2H]$^+$); calcd: 97.0766 ([M + H]$^+$), 98.0844 ([M + 2H]$^+$).

*2.2.2. Synthesis of 3,5-Diphenyl-1H-pyrazole, **L2**.* IR $\nu_{C=N}$ (cm^{-1}) = 1568, ν_{N-N} (cm^{-1}) = 1185; ^{13}C NMR ($CDCl_3$): δ_C(ppm) 154.2 (−C═N−), (−C−N−) 148.7, (−C═$C_{(aromatic)}$) 130.9, 128.8, 128.2, 127.3, 126.5, 125.7, (−C═C−$_{methine}$) 100.1; ^{1}H NMR (400 MHz, $CDCl_3$): δ_H (N−H) 10.96 (s, 1H), (−$CH_{(aromatic)}$) 7.78−7.23 (s, 5H), (−C═CH−) 6.76 (s, 1H); UV−vis: λ_{max} = 254 nm, ε [0.0005 M] = 1046 $M^{-1}\cdot cm^{-1}$, LC−MS: *m*/*z* = found: 221.1051 ([M + H]$^+$), 222.1132 ([M + 2H]$^+$); calcd: 221.1079 ([M + H]$^+$), 222.1157 ([M + 2H]$^+$).

*2.2.3. Synthesis of 3-(Trifluoromethyl)-5-phenyl-1H-pyrazole, **L3**.* IR $\nu_{C=N}$ (cm^{-1}) = 1509, ν_{N-N} (cm^{-1}) = 1117; ^{13}C NMR ($CDCl_3$): δ_C (ppm) (−C═N−) 145.1, (−C═C−$_{(aromatic)}$) 129.4, 129.3, 127.9, 125.6, 122.4, 119.7, (═C−$_{(methine)}$) 101.2; ^{1}H NMR (400 MHz, $CDCl_3$): δ_H (N−H) 9.32 (s, 1H), (C−$H_{(aromatic)}$) 7.62−7.34 (m, 4H), (═$CH_{(aromatic)}$−) 6.73 (s, 1H); UV−vis: λ_{max} = 252 nm, ε [0.0008 M] = 1029 $M^{-1}\cdot cm^{-1}$, LC−MS: *m*/*z* − found: 213.0665 ([M + H]$^+$), 214.0687 ([M + 2H]$^+$); calcd: 213.0640 ([M + H]$^+$), 214.0718 ([M + 2H]$^+$).

*2.2.4. Synthesis of 3-(Trifluoromethyl)-5-methyl-1H-pyrazole, **L4**.* IR $\nu_{C=N}$ (cm^{-1}) = 1587, ν_{N-N} (cm^{-1}) − 1121; ^{13}C NMR ($CDCl_3$): δ_C (ppm) (−C═N−) 143.2, 142.70, 141.24 (CF_3) 122.7, (−C═C−$_{(methine)}$)103.0, (−CH_3) 10.5; ^{1}H NMR (400 MHz, $CDCl_3$): δ_H (N−H) 10.98 (s, 1H), (−C═CH−$_{(methine)}$) 6.31 (s, 1H), (−CH_3) 2.34 (s, 3H); UV−vis: λ_{max} = 218 nm, ε [0.0011 M] − 685 $M^{-1}\cdot cm^{-1}$, LC−MS: *m*/*z* = found: 151.0456 ([M + H]$^+$), 152.0512 ([M + 2H]$^+$); calcd: 151.0483 ([M + H]$^+$), 152.0561 ([M + 2H]$^+$).

*2.2.5. Synthesis of 3,5-Ditert-butyl-1H-pyrazole, **L5**.* IR $\nu_{C=N}$ (cm^{-1}) − 1587, ν_{N-N} (cm^{-1}) = 1129; ^{13}C NMR (DMSO-d_6): δ_C (ppm) (−C═N−) 160.5, (−C═C−$_{(methine)}$) 96.8; C(CH_3) 30.9; ^{1}H NMR (400 MHz, $CDCl_3$): δ_H (N−H) 12.00 (s, 1H), (−C═CH−$_{(methine)}$) 5.82 (s, 1H), (−CH_3) 1.22 (s, 18H); UV−vis: λ_{max} = 282 nm, ε [0.0007 M] = 685 $M^{-1}\cdot cm^{-1}$, LC−MS: *m*/*z* = found: 181.1694 ([M + H]$^+$), 182.1763 ([M + 2H]$^+$); calcd: 181.1705 ([M + H]$^+$), 182.1783 ([M + 2H]$^+$).

2.3. Single-Crystal X-ray Crystallography. A single crystal of the synthesized pyrazole compound, **L1**, was analyzed on a Rigaku XtaLab Synergy R diffractometer, with a rotating-anode X-ray source and a HyPix CCD detector. Data reduction and absorption were carried out using the CrysAlisPro (version 1.17.40.23a) software.[28] X-ray diffraction measurement was performed at 150.00(2) K, using an Oxford Cryogenics Cryostat. The structure was solved by intrinsic

https://doi.org/10.1021/acsomega.5c00320
ACS Omega 2025, 10, 12671−12678

phasing with SHELXTS-2013[29] and refined using the SHELXL-2013[29] algorithm. All H atoms were placed in geometrically idealized positions and were constrained to ride on their parent atoms. The X-ray crystallographic coordinates for **L1** have been deposited at the Cambridge Crystallographic Data Centre (CCDC), with deposition number CSD: 2235800. The data can be obtained free of charge from the Cambridge Crystallographic Data Centre via www.ccdc.cam.ac.uk/data_request/cif.

2.4. Biological Studies. *2.4.1. Cell Culture.* The human PANC-1 pancreatic cancer (PC) cell line, MDA-MB-231 triple-negative breast cancer (BC) cells, and HeLa (HPV-18) cervical cancer (CC) cell line were grown in Dulbecco's modified Eagle's medium (DMEM) (Gibco, Life Technologies, New York). The CFPAC-1 PC cells were grown in Iscove's modified Dulbecco's medium (IMDM), and the CaSki (HPV-16) CC and MCF-7 (estrogen receptor-positive) BC cell lines were grown in Roswell Park Memorial Institute medium (RPMI) (Gibco, Life Technologies, New York). The culture media were supplemented with 10% fetal bovine serum (FBS) and 100 U/ml penicillin and 100 μg/mL streptomycin. All cells were cultured at 37 °C in a 5% CO_2-95% air-humidified incubator. Media were replaced every 2−3 days, and cells were routinely subjected to mycoplasma tests. Only mycoplasma-free cells were used in the experiments.

2.4.2. Cell Treatments. The compounds, **L1**−**L5**, were dissolved in dimethyl sulfoxide (DMSO) (Merck 48856212719) to achieve a stock concentration of 5 mM and subsequently stored at −20 °C for a maximum of 5 days before use. For cell culture treatments, the 5 mM stock solutions were diluted to final concentrations of 10 μM using respective supplemented cell culture media, and the percentage of DMSO in the 10 μM concentration was prepared and used as a vehicle control. Cisplatin (Pfizer Ltd., New York, USA) was included and used as the positive control for MCF-7, MDA-MB-231, CaSki, and HeLa cells, while gemcitabine (Sigma-Aldrich, USA) was used as a positive control for CFPAC-1 and PANC-1 cells.

2.4.3. Short-Term Cell Viability Assay. The effects of the experimental compounds **L1**−**L5** on the viability of CFPAC-1 and PANC-1 PC cells, MDA-MB-231 and MCF-7 BC cells, and CaSki and HeLa CC cells were assessed using the 3-(4,5-dimethylthiazol-2-yl)-2,5-diphenyltrazolium bromide (MTT) assay (M21281G, Sigma-Aldrich), following the manufacturer's guidelines. Briefly, cells were seeded in 96-well plates, and 24 h later, they were treated with 10 μM of the experimental compounds or the vehicle (DMSO) for 48 h, followed by the addition of 10 μL of the 5 mg/mL MTT solution to each well and incubation for further 4 h at 37 °C. This was followed by the addition of 100 μL solubilization buffer (10% SDS in 0.01 M HCl) followed by overnight incubation at 37 °C. The spectrophotometric absorbance of the samples was determined at a wavelength of 595 nm using the Glomax plate reader (Promega, USA). The mean cell viability was calculated and expressed as a percentage of the vehicle control.

To determine the IC_{50} values of selected compounds (**L2**, **L3**, and **L4**), cells were seeded as above and treated with a range of concentrations (10−50 μM) of these compounds followed by MTT assays, as previously described. The IC_{50} values were determined using GraphPad Prism version 8.0 software (GraphPad Prism software, USA) from sigmoidal plots of data obtained from two independent experiments performed in quadruplicate.

2.4.4. Statistical Analysis. Data were obtained from three independent experimental repeats and analyzed by an unpaired parametric *t*-test using the GraphPad Prism version 8.0 software (GraphPad Prism software, USA). Error bars represent the standard deviation (SD), and significance was accepted at $*p < 0.05$, $**p < 0.01$, $***p < 0.001$, and $****p < 0.0001$.

2.5. Results and Discussion. *2.5.1. Synthesis.* Five pyrazole compounds, **L1**−**L5**, are reported in this study. The compounds were synthesized using a typical condensation reaction of hydrazine with various β-diketone derivatives (pentane-2,4-dione; 2,2,6,6-tetramethylheptane-3,5-dione; 1,1,1-trifluoropentane-2,4-dione; 1,5-diphenylacetylacetone; and 4,4,4-trifluoro-1-phenylbutane-1,3-dione) to investigate the biological activity that is believed to have been rendered by the pyrazole function within the heterocyclic ring. Experimental data of these compounds will be discussed in IR, UV−vis, ^{1}H and ^{13}C NMR, LC−MS, SC-XRD, and biological analysis sections. Table 1 represents the FT-IR data of **L1**−**L5**.

Table 1. FT-IR Stretching Frequency Data of L1−L5

functional group	IR stretching frequencies (cm^{-1})				
	L1	**L2**	**L3**	**L4**	**L5**
C−C	1422	1410	1426	1436	1415
C=N	1600	1568	1509	1587	1570
C−N	1307	1272	1253	1246	1256
N−N	1148	1185	1117	1121	1129

2.5.2. IR Characterization. In the FT-IR spectra (see Figure SI4a−e), all the synthesized pyrazole compounds show typical C=N stretching frequencies (medium peak) at 1600 cm^{-1} for **L1**, 1568 cm^{-1} for **L2**, 1509 cm^{-1} for **L3**, 1587 cm^{-1} for **L4**, and lastly, 1570 cm^{-1} for **L5**. All these stretching frequencies, impacted by respective substitution on the backbone of the pyrazole moiety, are in good agreement with other related IR data reported in the literature.[30−32] The presence of the medium peaks attributed to C−N stretching at a region ranging between 1307 and 1246 cm^{-1} further supports the formation of these compounds. The −C−C− stretching of **L3** (1426 cm^{-1}) and **L4** (1436 cm^{-1}) occurs more downfield as compared to the −C−C− of **L1** (1422 cm^{-1}), **L2** (1410 cm^{-1}), and **L5** (1415 cm^{-1}). This is due to the presence of electron-withdrawing atoms (fluorides) at the terminal carbons of the former pyrazole compounds (**L3** and **L4**).

2.5.3. UV−Vis Characterization. The UV−vis spectra of the pyrazole-based compounds under study in the exploited wavelength region (200−400 nm) are shown in Figure SI3a−e. The wavelength of maximum absorbance for all the compounds ranges from 218 to 254 nm with their corresponding calculated molar absorptivities (ε) ranging between 435 and 1045 $M^{-1}\cdot cm^{-1}$, respectively, to **L1** and **L2**. A red-shifted broad absorption band is observed around 250 nm on **L2** and **L3** spectra as compared to the narrow absorption profiles (around 218 nm) of **L1**, **L4**, and **L5**. The observed bathochromic shift in the λ_{max} from 218 to 250 nm is a sure indication of aromatic moieties on the compound backbone since **L1**, **L4**, and **L5** are free from phenyl scaffolds. Moreover, a weak secondary peak is observed around 200 nm for the UV−vis spectra of **L2** and **L3**. All these noticeable

https://doi.org/10.1021/acsomega.5c00320
ACS Omega 2025, 10, 12671−12678

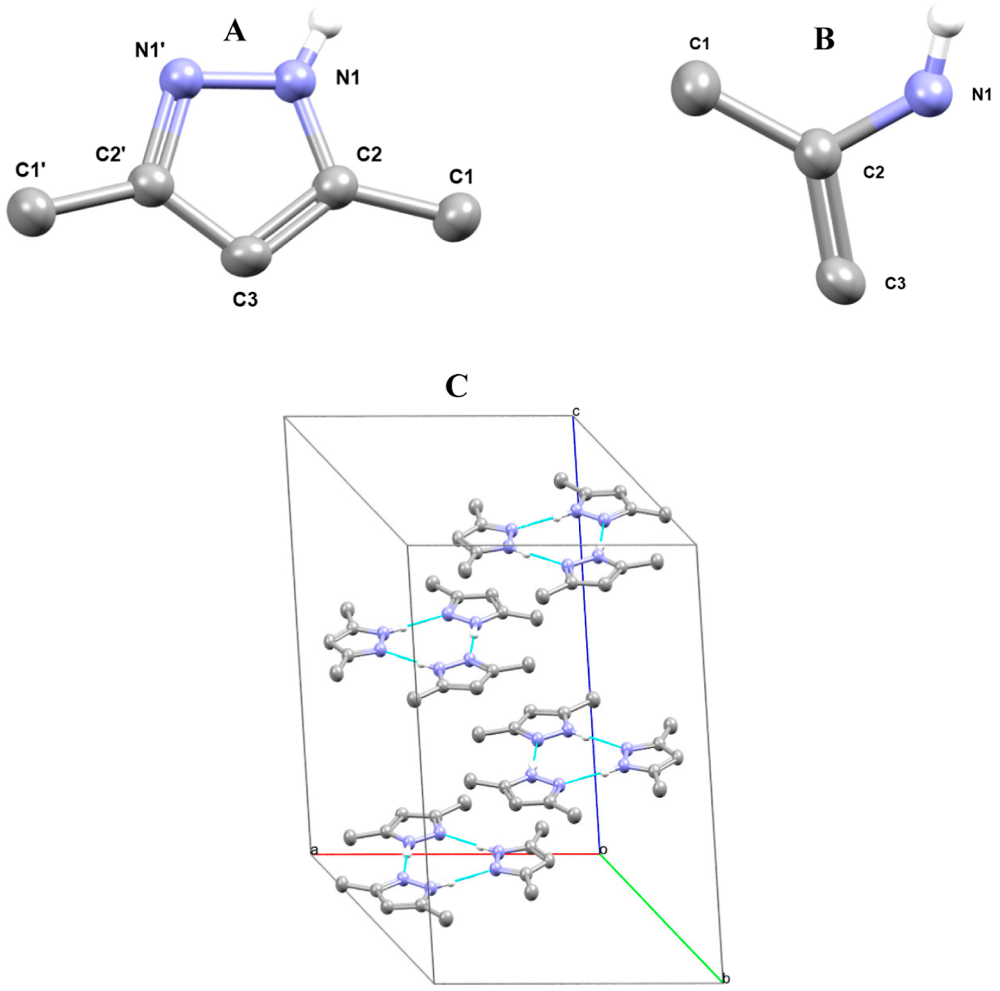

Figure 1. (A) Molecular structure of **L1**. Some hydrogen atoms are omitted for clarity, (B) asymmetric unit of the molecule, and (C) unit cell showing crystal packing and intermolecular hydrogen interactions. Thermal ellipsoids are displayed at 50% probability.

absorption profiles are characterized by $\pi-\pi^*$ (aromatic) transition according to the literature.[30]

2.5.4. NMR Characterization. The pyrazole compounds **L1**−**L5** are readily identified by their respective ^{1}H and ^{13}C NMR chemical shifts. The analyses for all of the compounds were done in $CDCl_3$ and DMSO solvents. All NMR data are consistent with the proposed structures and with other structures already reported in the literature.[30] In ^{13}C NMR, all these compounds, **L1**−**L5**, denote a downfield chemical shift (peak) at δ_C 144.2, 148.7, 145.1, 143.2, and 160.5 ppm, respectively, typically attributed to aromatic carbons within the pyrazole ring that are influenced by the adjacent nitrogen atoms, resulting in the carbon being deshielded and appearing downfield (C═N). In **L5**, the imine carbon signal (C═N) appears quite small; however, this could be due to the analysis time and also the amount of sample that was used for the ^{13}C NMR analysis (see Figure SI2b'). In the ^{1}H NMR spectra, a small prominent peak observed at δ_H 12.38, 10.96, 9.32, 10.98, and 11.20 ppm attributable to N−H for **L1**−**L5**, respectively, further advocates for the successful synthesis of these compounds. The methyl proton peaks for **L1** (2.31 ppm) and **L4** (2.34 ppm) are observed more downfield as compared to those of **L5** (1.15 ppm) and this might be due to the fact that the protons of the former (**L1** and **L4**) are much closer to the electron-withdrawing atoms (adjacent nitrogens) within the pyrazole moiety in contrast to the latter (**L5**).

2.5.5. Single-Crystal XRD Characterization. The molecular crystal structure of the pyrazole compound, **L1**, was validated by single-crystal X-ray diffraction. The solid-state molecular structures along with crystal packing with intermolecular hydrogen interactions of the pyrazole derivative mentioned above are shown in Figure 1. This compound crystallized in the trigonal crystal system within the $\bar{R}3c$ space group, corresponding to the previously determined structure of the same compound by Smith et al.[31] in 1989 at 295 K. In the structure reported herein, determined at 150 K, 36 molecules are present in the unit cell (Z = 36), and a head−head arrangement is noted in the packing of the molecules. In the asymmetric unit of **L1**, half a molecule exists, whereby a complete molecule is generated by means of a range of symmetry elements, including inversion center, rotation, and screw axes. The implication is that atoms C3, H3 (which resides on C3), and H1 (which resides on N1) are observed with associated 50% site occupancies to allow for a full occupancy in the grown structure (using the $2/3 - x$, $1/3 - x + y$, and $5/6 - z$ symmetry operator).

The molecular crystal structure consists of a heterocyclic moiety composed of three carbons and two adjacent nitrogen atoms, with methyl groups attached to the backbone of the molecule. The N1−N1′ bond distance is found to be 1.361(3) Å, while C1−C2 and C2−C3 bond distances are found to be 1.493(2) and 1.391(2) Å, respectively. On the other hand, the

https://doi.org/10.1021/acsomega.5c00320
ACS Omega 2025, 10, 12671−12678

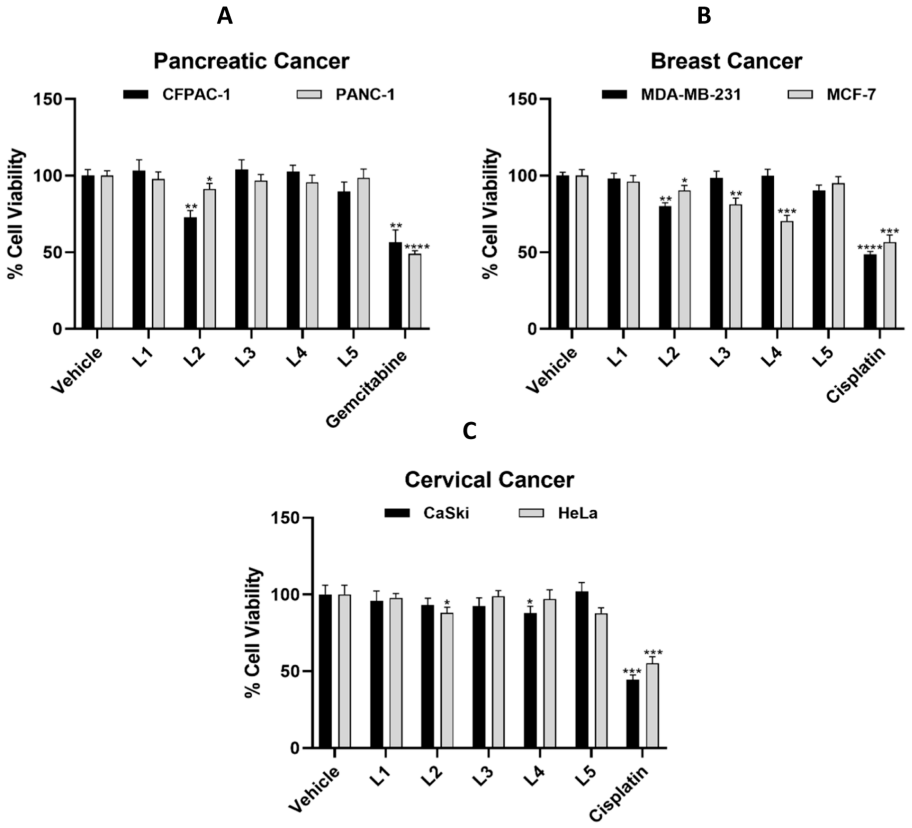

Figure 2. Single-dose treatments of pancreatic, breast, and cervical cancer cell lines with **L1−L5** compounds. (A) CFPAC-1 and PANC-1 pancreatic cancer, (B) MDA-MB-23 and MCF-7 breast cancer, and (C) CaSki and HeLa cervical cancer cell lines were treated with vehicle (DMSO) or 10 μM of L1-L5 for 48 h followed by MTT cell viability assay. Graphs represent the mean cell viability ± SD of three independent experiments performed in quadruplicate. Data were analyzed using the parametric unpaired *t*-test by GraphPad Prism 8.0 software where *p < 0.05, **p < 0.01, ***0.001, and ****0.0001.

Table 2. Summary of Percentage Viability 48 h Post-treatment with 10 μM of L1−L5 in Various Cancer Cell Lines

compounds	CFPAC-1	PANC-1	MDA-MB-231	MCF-7	CaSki	HeLa
vehicle	100 ± 3.98	100 ± 3.18	100 ± 2.14	100 ± 3.92	100 ± 6.05	100 ± 6.00
L1	103.39 ± 6.87	97.81 ± 4.62	98.00 ± 3.54	96.02 ± 4.01	95.93 ± 6.35	97.87 ± 2.84
L2	72.84 ± 4.31	91.31 ± 3.65	80.02 ± 2.29	90.36 ± 3.23	93.17 ± 4.40	88.09 ± 3.63
L3	104.10 ± 6.20	96.74 ± 3.94	98.42 ± 4.46	81.14 ± 4.14	92.52 ± 5.34	98.94 ± 3.68
L4	102.70 ± 4.05	95.64 ± 4.65	99.89 ± 4.30	70.30 ± 3.82	87.91 ± 4.40	97.08 ± 5.96
L5	89.74 ± 6.05	98.54 ± 5.75	90.47 ± 3.38	95.07 ± 4.25	102.09 ± 5.78	87.83 ± 3.45
gemcitabine	56.73 ± 7.79	49.10 ± 7.84				
cisplatin			48.63 ± 1.99	56.71 ± 4.45	44.41 ± 3.18	55.16 ± 4.22

C2−N1 and C2′═N1′ are both reported as 1.342(2) Å. This is due to the 50% probability of double bond tautomerism happening within the pyrazole ring. In comparison, the bond distances of the reported structure are in good agreement with other pyrazole compounds already reported in the literature.[32−35] Figure 1 and Table SI3 show that this compound is further stabilized by intermolecular hydrogen bonding (N−H···N), with a bond distance of 2.03(4) Å.

2.5.6. In Vitro Studies of Pyrazole Compounds. The treatment of most diseases remains an imperative and strenuous matter due to many issues associated with therapy. This includes the resistance of these diseases to currently known drugs and the rapid increase in virus and bacterial infections in immunoarbitrated patients (e.g., AIDS and cancer) after organ transplantation or during chemotherapy.[36−38] Despite the existence of many groups of compounds with various biological activities, pyrazole compounds are comprehensively explored because they are rich in pharmacological activity to most diseases.[39,40] Therefore, the cytotoxic effect of **L1−L5** pyrazole compounds was investigated in pancreatic (CFPAC-1 and PANC-1), breast (MDA-MB-231 and MCF-7), cervical (CaSki), and HeLa cancer cell lines. To this end, the cells were treated for 48 h with vehicle (DMSO) or 10 μM of the **L1−L5** compounds followed by MTT assays. Cisplatin and gemcitabine were included in these assays as reference drugs because they are used as a chemotherapeutic for these cancers.

In pancreatic cancer cell lines, compared to gemcitabine which showed a cell viability of 56.7% and 49.10% in CFPAC-1 and PANC-1 cells, respectively, none of the experimental compounds inhibited cell viability by more than 50%. However, **L2** was the most promising compound, which showed a significant inhibition of cell viability in both cell lines, i.e., 72.8% for CFPAC-1 and 91.31% for PANC-1 cells (Figure

https://doi.org/10.1021/acsomega.5c00320
ACS Omega 2025, 10, 12671−12678

Table 3. IC_{50} Values (μM) Determined for the Most Active Compounds, L2−L4, in Pancreatic and Breast Cancer Cell Lines[a]

cell lines		compound IC_{50} ± SD (μM)				
		L2	L3	L4	cisplatin[41]	gemcitabine[42]
pancreatic cancer	CFPAC-1	61.7 ± 4.9	–	–	–	1.5 ± 0.84
	PANC-1	104.7 ± 7.3	–	–	–	5.7 ± 0.19
breast cancer	MDA-MB-231	189.3 ± 0.87	–	–	13.98	–
	MCF-7	–	81.48 ± 0.89	185.5 ± 0.95	5.54	–

[a]NB: dashes (−) show that the compounds did not show significant cell viability on those specific cancer cell lines to be further screened in IC_{50} concentrations.

2A). As shown in Figure 2B, while compound **L2** significantly inhibited the viability of both MDA-MB-231 (80.02%) and MCF-7 (90.36%) cells, **L3** and **L4** showed a statistically significant inhibition of cell viability (81.14% and 70.3%, respectively) in the estrogen receptor-positive MCF-7 cell line. However, none of the compounds inhibited cell viability by more than 50% or was more effective than cisplatin in the breast cancer cell lines tested. Similarly, none of the compounds were more effective than cisplatin in cervical cancer cell lines, but compounds **L2** and **L4** showed promising results in HeLa (88.09%) and CaSki (87.91%) cells, respectively (Figure 2C). Overall, the results summarized in Table 2 reveals that although **L1**−**L5** were not as cytotoxic as the gold standard drugs gemcitabine and cisplatin, **L2** showed promise across all of the cancer cell lines tested. These results are consistent with numerous literature reports on the potential biological activity of pyrazole compounds on various cancer cell lines.[35−39]

We therefore determined the half maximal inhibitory (IC_{50}) concentrations of **L2**, **L3**, and **L4** in the cancer cell lines where they showed most activity, and their results are listed in Table 3. Our results showed that **L2** exhibited IC_{50} values of 61.7 and 104.7 μM in the CFPAC-1 and PANC-1 pancreatic cancer cell lines, respectively, and 189.3 μM in the MDA-MB-231 triple negative breast cancer cells. In the estrogen receptor positive MCF-7 breast cancer cells, IC_{50} values of 81.5 and 185.5 μM were obtained for **L3** and **L4**, respectively. The IC_{50} values obtained for our compounds are much greater than those of cisplatin and gemcitabine, which are our reference standards, with IC_{50} values of 13.98 and 5.54 μM against

MDA-MB-231 and MCF-7 breast cancers for cisplatin and 1.5 ± 0.84 and 5.7 ± 0.19 μM against CFPAC-1 and PANC-1 pancreatic cancers for gemcitabine. Graphical representation of the results obtained is illustrated in the Supporting Information (Figure SI6).

2.6. Conclusions. In this study, five pyrazole compounds (**L1**−**L5**) were synthesized and analyzed by using FT-IR, ^{1}H and ^{13}C NMR, UV−vis, LC−MS, and single-crystal X-ray crystallography techniques. The short-term cytotoxicity of the synthesized pyrazole compounds was explored on CFPAC-1, PANC-1, MDA-MB-231, MCF-7, CaSki, and HeLa cancer cell lines via the MTT viability assay. Based on the outcomes obtained from anticancer screening, it is evident that none of the compounds exhibited more activity than the standard drugs in the cancer cell lines tested, which is the main limitation to this study. However, **L2** showed the most promising outcome against pancreatic (CFPAC-1) cancer with IC_{50} value of 61.7 ± 4.9 μM. Therefore, further investigation such as coordinating these compounds to *d*-group metals (Re, Tc, and Mn) to evaluate their biological behavior remains to be investigated for drug discovery and development in the future. These pyrazole moieties can also be explored biologically on other diseases such malaria, TB, and Chagas disease.

■ ASSOCIATED CONTENT

Supporting Information

The Supporting Information is available free of charge at https://pubs.acs.org/doi/10.1021/acsomega.5c00320.

Crystallographic data; selected bond lengths and angles; hydrogen interactions; ^{1}H and ^{13}C NMR spectra of **L1**−**L5**; UV−vis spectra; IR spectra; MS spectra; and half-maximal inhibitory (IC_{50}) concentrations of **L2**, **L3**, and **L4** (PDF)

■ AUTHOR INFORMATION

Corresponding Author

Amanda-Lee E. Manicum − *Department of Chemistry, Tshwane University of Technology, Pretoria 0001, South Africa;* orcid.org/0000-0003-4064-1307; Email: manicumAE@tut.ac.za

Authors

Lesetja V. Ramoba − *Department of Chemistry, Tshwane University of Technology, Pretoria 0001, South Africa;* orcid.org/0000-0001-9510-1258

Wakopo J. Nzondomyo − *Department of Chemistry, Tshwane University of Technology, Pretoria 0001, South Africa*

Karabo Serala − *Department of Human Biology, University of Cape Town, Cape Town 7925, South Africa*

Lucy W. Macharia − *Department of Human Biology, University of Cape Town, Cape Town 7925, South Africa*

Supratim Biswas − *Department of Human Biology, University of Cape Town, Cape Town 7925, South Africa*

Sharon Prince − *Department of Human Biology, University of Cape Town, Cape Town 7925, South Africa*

Frederick P. Malan − *Department of Chemistry, University of Pretoria, Pretoria 0001, South Africa*

Orbett T. Alexander − *Department of Chemistry, University of the Western Cape, Cape Town 7535, South Africa*

Complete contact information is available at: https://pubs.acs.org/10.1021/acsomega.5c00320

Notes

The authors declare no competing financial interest.

■ ACKNOWLEDGMENTS

This work is based on the research supported by the National Research Foundations of South Africa under the Thuthuka programme (Grant specific unique reference numbers 113629). We would like to express our gratitude toward the Tshwane University of Technology together with the Department of Chemistry for institutional support and the University

of Pretoria for crystal data collection and refinements. The authors acknowledge that the opinions, findings, conclusions, or recommendations expressed in this publication do not necessarily reflect the views of the SA National Research Foundation.

REFERENCES

(1) Knorr, L. Einwirkung von acetessigester auf phenylhydrazin. *Ber. Dtsch. Chem. Ges.* **1883**, *16* (2), 2597−2599.
(2) Girish, Y. R.; Kumar, K. S. S.; Manasa, H. S.; Shashikanth, S. ZnO: An Ecofriendly, Green Nano-catalyst for the Synthesis of Pyrazole Derivatives under Aqueous Media. *JCCS* **2014**, *61* (11), 1175−1179.
(3) Huang, Y. R.; Katzenellenbogen, J. A. Regioselective synthesis of 1, 3, 5-triaryl-4-alkylpyrazoles: novel ligands for the estrogen receptor. *Org. Lett.* **2000**, *2* (18), 2833−2836.
(4) El Ghomari, M. J.; Mokhlisse, R.; Laurence, C.; Le Questel, J. Y.; Berthelot, M. Basicity of azoles: complexes of diiodine with imidazoles, pyrazoles, and triazoles. *J. Phys. Org. Chem.* **1997**, *10* (9), 669−674.
(5) Abboud, J. L. M.; Cabildo, P.; Canada, T.; Catalan, J.; Claramunt, R. M.; De Paz, J. L. G.; Elguero, J.; Homan, H.; Notario, R. Basicity of C-substituted pyrazoles in the gas phase: an experimental (ICR) and theoretical study. *J. Org. Chem.* **1992**, *57* (14), 3938−3946.
(6) Taft, R. W.; Anvia, F.; Taagepera, M.; Catalan, J.; Elguero, J. Electrostatic proximity effects in the relative basicities and acidities of pyrazole, imidazole, pyridazine, and pyrimidine. *J. Am. Chem. Soc.* **1986**, *108* (12), 3237−3239.
(7) Plem, S. C.; Müller, D.; Murguia, M. C. Key intermediates: a simple and highly selective synthesis of 5-amino-1-aryl-1H-pyrazole-4-carbonitriles for applications in the crop protection. *Adv. Chem. Eng. Sci.* **2015**, *5*, 239−261.
(8) Vitor, R. F.; Alves, S.; Correia, J. D. G.; Paulo, A.; Santos, I. Rhenium (I)-and technetium (I) tricarbonyl complexes anchored by bifunctional pyrazole-diamine and pyrazole-dithioether chelators. *J. Org. Chem.* **2004**, *689* (25), 4764−4774.
(9) Chkirate, K.; Essassi, E. M. Pyrazole and benzimidazole derivatives: chelating properties towards metals ions and their applications. *Curr. Org. Chem.* **2023**, *26* (19), 1735−1766.
(10) Roozemond, D. A.; Den Hond, F.; Veldhuis, J. B. J.; Strasdeit, H.; Driessen, W. L. Preferred uptake of Cu (II) and Cd (II) by novel pyrazole-functionalized chelating polymers. *Eur. Polym. J.* **1988**, *24* (9), 867−872.
(11) Verma, G.; Marella, A.; Shaquiquzzaman, M.; Akhtar, M.; Ali, M. R.; Alam, M. M. A review exploring biological activities of hydrazones. *J. Pharm. BioAllied Sci.* **2014**, *6* (2), 69−80.
(12) Rollas, S.; Güniz Küçükgüzel, S. . Biological activities of hydrazone derivatives. *Molecules* **2007**, *12* (8), 1910−1939.
(13) de Oliveira Carneiro Brum, J.; França, T. C.; LaPlante, S. R.; Villar, J. D. F. Synthesis and biological activity of hydrazones and derivatives: A review. *Mini-Rev. Med. Chem.* **2020**, *20* (5), 342−368.
(14) Keter, F. K.; Darkwa, J. Perspective: the potential of pyrazole-based compounds in medicine. *BioMetals* **2012**, *25*, 9−21.
(15) Malinowska, K.; Lorenz, I. P.; Sadowska, B.; Mucha, P. Metal ion complexes with pyrazoles, aziridines and diaziridines−synthesis and biological activity. *Curr. Med. Chem.* **2019**, *26* (4), 648−663.
(16) Abrigach, F.; Touzani, R. Pyrazole derivatives with NCN junction and their biological activity: A review. *Med. Chem.* **2016**, *06*, 292−298.
(17) Ardiansah, B. Recent reports on pyrazole-based bioactive compounds as candidate for anticancer agents. *Asian J. Pharm. Clin. Res.* **2017**, *12* (45.10), 22159.
(18) Liang, Z.; Rong, Z.; Cong, H.; Qing-Ying, D.; Ming-Zhu, S.; Jie, W.; Xu-Liang, N.; Jin-Zhu, C.; Shang-Xing, C.; Da-Yong, P. Design, synthesis and antifungal activity of novel pyrazole amides derivates. *J. Mol. Struct.* **2023**, *1277*, 134881.
(19) Qiao, L.; Zhai, Z. W.; Cai, P. P.; Tan, C. X.; Weng, J. Q.; Han, L.; Liu, X.; Zhang, Y. Synthesis, crystal structure, antifungal activity, and docking study of difluoromethyl pyrazole derivatives. *J. Heterocycl. Chem.* **2019**, *56* (9), 2536−2541.
(20) Bekhit, A. A.; Ashour, H. M.; Guemei, A. A. Novel pyrazole derivatives as potential promising anti-inflammatory antimicrobial agents. *Arch. Pharm. Int. J. Pharm. Med. Chem.* **2005**, *338* (4), 167−174.
(21) Mantzanidou, M.; Pontiki, E.; Hadjipavlou-Litina, D. Pyrazoles and pyrazolines as anti-inflammatory agents. *Molecules* **2021**, *26* (11), 3439.
(22) Liu, J. J.; Zhao, M. Y.; Zhang, X.; Zhao, X.; Zhu, H. L. Pyrazole derivatives as antitumor, anti-inflammatory and antibacterial agents. *Mini Rev. Med. Chem.* **2013**, *13* (13), 1957−1966.
(23) A Alam, M. Antibacterial pyrazoles: Tackling resistant bacteria. *Future Med. Chem.* **2022**, *14* (5), 343−362.
(24) Liu, J. J.; Zhang, H.; Sun, J.; Wang, Z. C.; Yang, Y. S.; Li, D. D.; Zhang, F.; Gong, H. B.; Zhu, H. L. Synthesis, biological evaluation of novel 4, 5-dihydro-2H-pyrazole 2-hydroxyphenyl derivatives as BRAF inhibitors. *Bioorg. Med. Chem. Lett.* **2012**, *20* (20), 6089−6096.
(25) Rong, N.; Qiu, T.; Qian, R.; Lü, L.; Huang, X.; Ma, Z.; Cui, C. Three pyrazole-3-carboxylic acid complexes as efficient solvent-free heterogeneous catalysts for CC bond formation. *Inorg. Chem. Commun.* **2017**, *86*, 98−104.
(26) Modi, C. K.; Vithalani, R. S.; Patel, D. S.; Som, N. N.; Jha, P. K. Zeolite-Y entrapped metallo-pyrazolone complexes as heterogeneous catalysts: Synthesis, catalytic aptitude and computational investigation. *Microporous Mesoporous Mater.* **2018**, *261*, 275−285.
(27) Silva, T. F.; Leod, T. C. M.; Martins, L. M.; Guedes da Silva, M. F. C.; Schiavon, M. A.; Pombeiro, A. J. Pyrazole or tris(pyrazolyl)-ethanol oxo-vanadium(IV) complexes as homogeneous or supported catalysts for oxidation of cyclohexane under mild conditions. *J. Mol. Catal. A: Chem.* **2013**, *367*, 52−60.
(28) Rigaku, O. D. *CrysAlis PRO Software system*; Rigaku Corporation, 2018.
(29) Sheldrick, G. M. Crystal Structure Refinement with SHELXL. *Acta Crystallogr., Sect. C: Struct. Chem.* **2015**, *71* (1), 3−8.
(30) Faundez-Gutierrez, R.; Macleod-Carey, D.; Zarate, X.; Bustos, C.; Molins, E.; Schott, E. Synthesis, characterization and DFT study of a new family of pyrazole derivatives. *Polyhedron* **2014**, *81*, 414−420.
(31) Smith, J. A. S.; Wehrle, B.; Aguilar-Parrilla, F.; Limbach, H. H.; Foces-Foces, M. d. l. C.; Hernandez Cano, F.; Elguero, J.; Baldy, A.; Pierrot, M.; Khurshild, M. M. T.; Larcombe-McDouall, J. B. Intermolecular Triple Proton and Deuteron Transfer in Crystalline 3,5-Dimethylpyrazóle Studied by NMR, NQR, and X-ray Methods. *J. Am. Chem. Soc.* **1989**, *111*, 7304−7312.
(32) de Sousa, G. F.; Gatto, C. C.; Resck, I. S.; Deflon, V. M. Synthesis, spectroscopic studies and X-ray crystal structures of new pyrazoline and pyrazole derivatives. *J. Chem. Crystallogr.* **2011**, *41*, 401−408.
(33) Zhang, J.; Tan, D. J.; Wang, T.; Jing, S. S.; Kang, Y.; Zhang, Z. T. Synthesis, crystal structure, characterization and antifungal activity of 3, 4-diaryl-1H-Pyrazoles derivatives. *J. Mol. Struct.* **2017**, *1149*, 235−242.
(34) Mahmudov, I.; Ibrahimova, B.; Taslimi, P.; Sadeghian, N.; Karaoğlan, Z.; Taskin-Tok, T.; Abdullayev, Y.; Farzaliyev, V.; Sujayev, A.; Alwasel, S. H.; et al. Synthesis, characterization, crystal structure, molecular docking, and biological studies of Cu, Ni and Co metal complexes of pyrazole. *J. Mol. Struct.* **2024**, *1309*, 138205.
(35) Hassan, A. S.; Moustafa, G. O.; Askar, A. A.; Naglah, A. M.; Al-Omar, M. A. Synthesis and antibacterial evaluation of fused pyrazoles and Schiff bases. *Synth. Commun.* **2018**, *48* (21), 2761−2772.
(36) Morsy, N. M.; Hassan, A. S.; Hafez, T. S.; Mahran, M. R.; Sadawe, I. A.; Gbaj, A. M. Synthesis, antitumor activity, enzyme assay, DNA binding and molecular docking of Bis-Schiff bases of pyrazoles. *J. Iran. Chem. Soc.* **2021**, *18*, 47−59.
(37) Titi, A.; Messali, M.; Alqurashy, B. A.; Touzani, R.; Shiga, T.; Oshio, H.; Fettouhi, M.; Rajabi, M.; Almalki, F. A.; Ben Hadda, T.

https://doi.org/10.1021/acsomega.5c00320
ACS Omega 2025, 10, 12671−12678

Synthesis, characterization, X-Ray crystal study and bioctivities of pyrazole derivatives: Identification of antitumor, antifungal and antibacterial pharmacophore sites. *J. Mol. Struct.* **2020**, *1205*, 127625.
(38) Kumar, A. D.; Vivek, H. K.; Srinivasan, B.; Naveen, S.; Kumara, K.; Lokanath, N. K.; Byrappa, K.; Kumar, K. A. Design, synthesis, characterization, crystal structure, Hirshfeld surface analysis, DFT calculations, anticancer, angiogenic properties of new pyrazole carboxamide derivatives. *J. Mol. Struct.* **2021**, *1235*, 130271.
(39) Chauhan, S.; Paliwal, S.; Chauhan, R. Anticancer activity of pyrazole via different biological mechanisms. *Synth. Commun.* **2014**, *44* (10), 1333−1374.
(40) Bouabdallah, I.; M'Barek, L. A.; Zyad, A.; Ramdani, A.; Zidane, I.; Melhaoui, A. Anticancer effect of three pyrazole derivatives. *Nat. Prod. Res.* **2006**, *20* (11), 1024−1030.
(41) Benamrane, A.; Herry, B.; Vieru, V.; Chakraborty, S.; Biswas, S.; Prince, S.; Marschner, C.; Blom, B. Ionic ruthenium and iron based complexes bearing silver containing anions as a potent new class of anticancer agents. *J. Organomet. Chem.* **2021**, *934*, 121659.
(42) Serala, K.; Bai, J.; Prince, S. Pyrvinium Pamoate Alone and With Gemcitabine Exhibits Anti-Pancreatic Cancer Activity in 2D and 3D Cell Culture Models. *J. Cell. Mol. Med.* **2024**, *28* (23), No. e70222.

https://doi.org/10.1021/acsomega.5c00320
ACS Omega 2025, 10, 12671−12678